

V International Scientific and Technical Conference Actual Issues of Power Supply Systems

Active Experimental Evaluation of Motor Load Power Characteristics in the Presence of High Harmonics

AIPCP25-CF-ICAIPSS2025-00089 | Article

PDF auto-generated using **ReView**



Active Experimental Evaluation of Motor Load Power Characteristics in the Presence of High Harmonics

Ulugbek Ruziyev ^{a)}, Uchkun Eshonkulov, Najmiddin Boymurodov, Asliddin Abduazizov, Khujakulov Amirjon

Karshi State Technical University, Karshi, Uzbekistan

^{a)} Corresponding author: ulugruziyev2@gmail.com

Abstract: The article examines the problems of constructing static load characteristics under conditions of high harmonic distortion. Mathematical expressions for calculating power components in the presence of higher-order harmonics are proposed. Reactive power is determined at the fundamental frequency based on minimizing the computational error of electronic energy meters and ensuring the lowest possible cost for achieving maximum reactive power compensation using capacitor banks. The dependences between distortion power and voltage are obtained from measurements conducted on a laboratory test bench. These dependencies make it possible to identify the nature and sources of harmonic distortion, as well as to develop measures aimed at reducing distortion power and minimizing the consumers' contribution to voltage distortion.

INTRODUCTION

Electric power consumers include industrial, residential, and transport sectors, among which asynchronous motors dominate due to their continuous reactive power demand. With the expansion of electrification and nonlinear devices, the reactive component of modern loads has significantly increased, complicating power factor management and voltage stability in distribution networks [1].

In modern power systems, nonlinear loads such as rectifiers and frequency converters introduce harmonic currents that distort voltage and current waveforms, affecting both power quality and reactive power balance [2].

In addition, the share of specialized power consumers is steadily expanding. These include rectifier and inverter systems, electrochemical and electrometallurgical equipment, such as electrolytic cells and electric arc furnaces, and electrically powered transport infrastructure including railways and urban transit systems [3]. Collectively, these categories contribute to the complexity of load management and reactive power compensation within modern power networks. It is also noteworthy that transmission and distribution losses account for a substantial fraction of total electricity consumption, emphasizing the need for enhanced energy efficiency and optimized power factor correction in all sectors of electricity use [4].

The principal feature defining an electrical consumer load is its active and reactive power consumption. The amount of power drawn by a load is determined primarily by the supply voltage and frequency. The static load characteristics $P_H(U)$, $Q_H(U)$ or $P_H(f)$, $Q_H(f)$ present the dependence of active and reactive power on voltage or frequency under conditions of slow variations in operating parameters [5]. Such variations occur gradually enough for each operating point to correspond to a steady-state condition of the system [6].

In contrast, dynamic load characteristics describe the same relationships under conditions of rapid changes in voltage or frequency, reflecting transient processes in the power system and accounting for the rate of parameter variation.

The active power of the load is generally independent of frequency and, under the assumption that the resistance $r_H = const$, it is directly proportional to the square of the supply voltage.

Mathematically, this relationship can be expressed as:

$$P = U^2/r_p = U^2 \quad (1)$$

Considering the nonlinear relationship between the filament resistance of incandescent lamps and the applied voltage, the active power consumed by the lighting load exhibits a proportional dependence on the voltage raised to the exponent of 1.6 [7]. This relationship defines the static characteristic of the active power as a function of the supply voltage, as illustrated in Figure 1.

The characteristic approximate composition of the complex load for the electrical systems of our country, expressed as a percentage, is provided below:

TABLE 1. Approximate composition of electrical load categories in power systems

N _o	Category of electrical load	Approximate share, %
1	Small asynchronous motors	32–35
2	Large asynchronous motors	12–15
3	Lighting	23–27
4	Rectifiers, inverters, furnaces, and heating appliances	9–11
5	Synchronous motors	9–11
6	Network losses	7–9

An asynchronous motor consumes an amount of power that is practically equivalent to the power required by the driven working machine, assuming that the active power losses within the motor are negligible [8]. In general, working machines exhibit three principal types of mechanical characteristics: (a) a constant mechanical torque M_{mech} that remains independent of the angular velocity ω ; (b) a torque directly proportional to the angular velocity; and (c) a torque proportional to the square of the angular velocity [9].

Let us assume that the mechanical torque M_{mech} is independent of the parameter σ and, consequently, of the slip. Under this assumption, the mechanical power becomes directly proportional to the angular velocity, i.e., $P_{mech} \propto \omega$. The simplified L-shaped equivalent circuit of the asynchronous motor, which illustrates this relationship, is presented in Figure 2. It should be noted that this equivalent circuit neglects several secondary effects that have minimal influence on the overall energy conversion process [10].

Modern electrical power systems increasingly supply mixed nonlinear loads, including induction motors, rectifiers, and frequency-controlled drives, which produce significant harmonic distortion and reactive power demand [11]. These factors alter the voltage–power behavior of consumers and reduce the accuracy of classical static load models that assume purely sinusoidal conditions. As a result, the combined effect of voltage variation and harmonics on the active, reactive, and distortion power components of induction motor loads remains insufficiently understood [12].

This study aims to provide a comprehensive analysis of the static dependencies $P(U)$ and $Q(U)$ under harmonic distortion by integrating analytical modeling with experimentally validated data. Using the IEEE 1459–2010 power decomposition, the research establishes a more accurate representation of how harmonic content and voltage deviations jointly influence load characteristics [13].

The scientific novelty of the work lies in developing an analytical framework that adapts verified laboratory measurements for modeling harmonic-affected motor load behavior without requiring additional experiments. By explicitly incorporating distortion phenomena into the voltage–power relationships, the proposed approach offers an improved and practically applicable method for assessing reactive power, distortion power, and compensation effectiveness in networks with nonlinear loads [14].

The active power, calculated as a function of both voltage and slip based on the equivalent circuit presented in Figure 2, can be expressed as:

$$P = 3I^2 \frac{r_2}{s} = \frac{U^2}{(r_2/s)^2 + x_s^2} \frac{1_s}{s} = \frac{U^2 r_2 s}{r_2^2 + (x_s s)^2} \quad (2)$$

We will assume, as an approximation, that:

$$M_{mech} = \frac{P_{mech}}{\omega_0} = \frac{P}{\omega_0} = 3I^2 \frac{r_2}{s} \frac{1}{\omega_0} \quad (3)$$

Assuming that the mechanical torque M_{mech} remains constant and the normalized angular velocity $\omega_0 = 1$, it can be inferred that the relative values of torque and active power are equivalent ($P^* = M^*$). Based on the preceding expression, the following relationship is obtained:

$$3I^2 \frac{r_2}{s} = const, \quad (4)$$

that is, the slip is proportional to the square of the current:

$$S \equiv I^2 \quad (5)$$

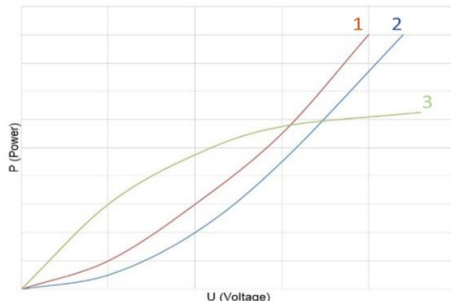


FIGURE 1. Static characteristics of the active power of a lighting load as a function of voltage $P(U)$:

1 – for $r_n = \text{const}$; 2 – for r_n dependent on U according to curve 3; 3 – dependence of the filament lamp resistance on voltage.

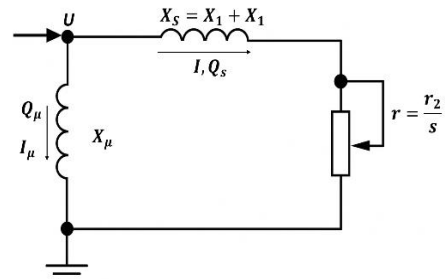


FIGURE 2. Simplified equivalent circuit of an asynchronous motor:

X_s - total leakage reactance of the stator winding (X_1) and the rotor winding (X_2);
 r_2 - rotor resistance referred to the stator, including the stator winding resistance.

Physically, when the supply voltage decreases below the critical value $U < U_{cr}$ the rotating motor begins to decelerate [8]. As a result, both the current and the reactive power increase sharply, and eventually, the motor comes to a stop—this phenomenon is referred to as motor stalling. Typically, electric motors operate with a significant stability margin, that is, well within their permissible operational range [15]. Only substantial voltage drops—on the order of 20–40% of the nominal voltage U_{nom} —can cause the motor to lose synchronism and stall.

The reactive power Q of the motor consists of two main components (see Fig. 2):

$$Q = Q_\mu + Q_s \quad (6)$$

where Q_μ is the magnetizing power associated with the magnetizing current I_μ , and Q_s represents the leakage power, i.e., the reactive power absorbed in the leakage reactance X_s .

The magnetizing power depends on the square of the supply voltage and can be expressed as

$$Q_\mu = \frac{U^2}{X_\mu} \quad (7)$$

In the case where X_μ remains constant, this relationship forms a parabolic dependence (see Fig. 4, curve 2). However, when X_μ decreases due to magnetic circuit saturation within the motor, the dependence of Q_μ deviates from the ideal parabolic form.

The power released in the leakage reactance X_s is proportional to the square of the current and can be expressed as

$$Q_s = 3I^2X_s \quad (8)$$

METHODS

The experimental and analytical part of this study was designed to investigate the behavior of induction motor loads under varying voltage and harmonic distortion conditions. The research utilized the active experimental method, which combines direct measurements of power parameters with computer-based modeling to validate theoretical assumptions. This approach allows for the comprehensive assessment of how supply voltage variations and harmonic components influence active, reactive, and distortion powers [16].

The reliability of the obtained results was ensured by performing simulation modeling and analytical validation using experimental data reported by Skamyin and Vasilkov. The simulation phase was implemented using the *SimPowerSystems* environment, where the electrical network, induction motor, and nonlinear loads were represented through equivalent circuit models. The laboratory setup was constructed to replicate realistic operating conditions and included the following main components: a three-phase autotransformer for voltage regulation, a three-phase induction motor mechanically coupled to a DC generator acting as the adjustable load, a capacitor bank equipped with an anti-harmonic reactor for reactive power compensation, and an uncontrolled three-phase rectifier with a resistive load for generating harmonic distortion [17].

Voltage at the motor terminals was varied smoothly from 180 V to 230 V in 10 V increments. At each voltage step, key electrical parameters — such as current, voltage, active power (P), reactive power (Q), total harmonic distortion of voltage (THDU), and current (THDI) — were recorded using a Resurs UF2M power quality analyzer with a measurement accuracy of $\pm 0.5\%$. Data processing and numerical calculations were performed in MATLAB, which enabled precise determination of static load characteristics and verification of theoretical relationships between voltage, power, and harmonic distortion.

The experimental program consisted of three modes. In the first mode, the induction motor was operated at no-load together with a rectifier connected to a resistive load. The second mode included an additional mechanical load applied to the motor shaft, while the third mode added a capacitor bank to the system for reactive power compensation. This arrangement made it possible to evaluate how reactive power, distortion power, and overall efficiency change depending on both the electrical and mechanical loading conditions [18].

The resulting datasets were used to construct the voltage–power dependencies $P(U)$ and $Q(U)$, as well as to analyze the influence of harmonic distortion on system stability and energy efficiency. The combined application of experimental measurement and numerical modeling ensured high accuracy of the results and provided a solid foundation for the subsequent discussion of static and dynamic characteristics of induction motor loads [19].

The mathematical framework follows the IEEE 1459–2010 decomposition of apparent power into active, reactive, and distortion components, which allows precise interpretation of voltage–power dependencies under harmonic conditions.

RESULTS AND DISCUSSIONS

The analysis of the obtained experimental and simulation data allowed for constructing the static load characteristics of nonlinear electrical systems under the influence of high harmonics. The research involved evaluating active, reactive, and distortion power components while varying the supply voltage in the range of 180–230 V.

Reactive power was determined according to the Kusters & Moore and IEEE 1459-2010 definitions, which provided the minimum computational error and ensured accurate assessment of compensation efficiency using condenser batteries. The obtained results confirmed that this method is the most appropriate for estimating reactive power and distortion components in the presence of harmonics [20].

Reactive and distortion power components were calculated for different operation modes of the system. The most significant parameters were obtained by comparing simulation and laboratory data for various nonlinear loads such as uncontrolled rectifiers and frequency-controlled drives.

$$S_N = S_1 (THD_1^2 + THD_U^2)^{0.5} \quad (9)$$

$$S_N = S_1 \cdot THDI \quad (10)$$

It was shown that distortion power can be effectively estimated using current harmonic distortion indices, with an error not exceeding 1%, thus enabling preliminary identification of the consumer's contribution to voltage distortion.

Experimental Results of Static Load Characteristics

Laboratory measurements were conducted using a three-phase autotransformer, induction motor with adjustable mechanical load, condenser battery, and nonlinear rectifier load. Measurements of voltage, current, active and reactive power, and total harmonic distortion were performed using the Resurs UF2M analyzer.

Three modes of operation were tested:

1. Induction motor (1.5 kW) operating at no-load with rectifier load (≈ 1.0 kW).
2. The same configuration with additional mechanical load.
3. Mode 2 plus a 1 kvar condenser battery for compensation.

TABLE 2. Simplified harmonic parameters of nonlinear loads

Type of nonlinear load	Harmonic number (n)	Current amplitude I_m (%)	Phase angle ψ_i (°)
Rectifier with RC load	3	80	135
Rectifier with L-filter	5	20	105
Frequency-controlled drive (0.5 kVA)	3	25	-110
Frequency-controlled drive with inductive filter	5	18	140

Based on these data, the voltage dependencies of active and reactive powers, $P(U)$ and $Q(U)$, were obtained using analytical simulation. These relationships follow the expected trend: active power increases approximately linearly with voltage, while reactive power shows a parabolic dependence [12].

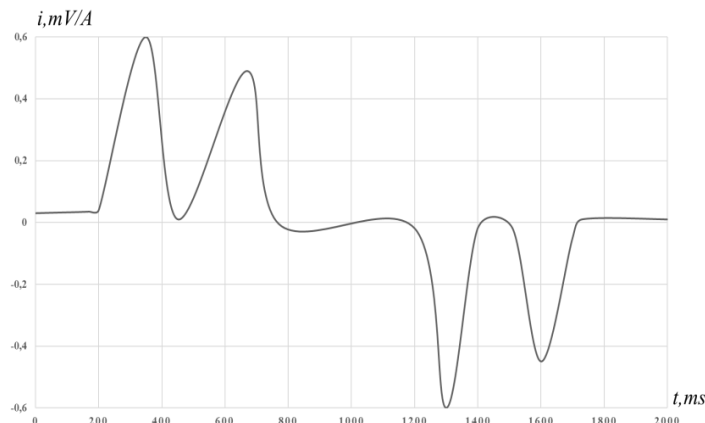


FIGURE 3. Instantaneous current waveform of an induction drive operating under variable mechanical load.

As seen from Fig. 3, the current waveform exhibits a pronounced nonsinusoidal profile with distinct harmonic distortion peaks corresponding to commutation effects in the rectifier circuit.

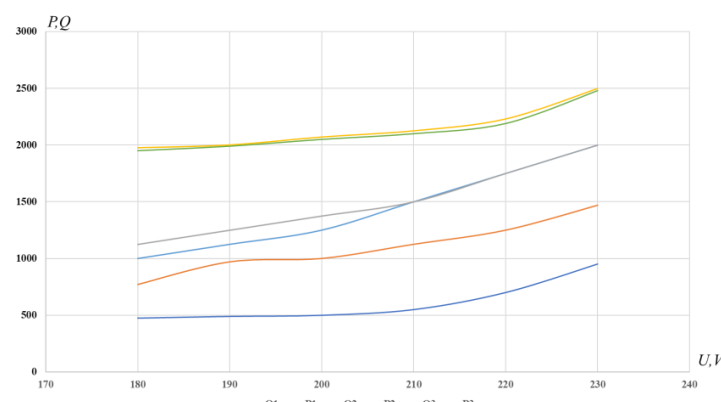


FIGURE 4. Static voltage-power characteristics $P(U)$ and $Q(U)$.

In contrast, the distortion power $D(U)$ exhibits a more complex nonlinear behavior correlated with THDI. When voltage decreases, THDU increases due to higher circuit impedance, while THDI changes irregularly depending on transformer saturation.

As shown in Fig. 3, the current waveform demonstrates notable nonsinusoidal distortion caused by commutation effects and harmonic interaction between the rectifier and motor drive. The harmonic spectrum is dominated by the 3rd and 5th orders, corresponding to the nonlinear switching pattern of the load.

The active power $P(U)$ shows an approximately linear dependence on supply voltage, while reactive power $Q(U)$ exhibits a quadratic trend, confirming the parabolic nature of magnetizing power described by Eq. (7).

Summary of Findings

1. Reactive power calculation according to IEEE 1459–2010 provides the most accurate and cost-effective estimation in harmonic conditions.
2. Distortion power can be used to identify each consumer's contribution to total voltage distortion at the PCC.
3. The addition of condenser batteries significantly affects the direction and magnitude of distortion power variation, demonstrating the need for optimized compensation strategies.

These findings validate the applicability of IEEE 1459–2010 definitions for practical estimation of harmonic power components and confirm that the use of condenser banks can improve overall power factor without significantly increasing distortion power.

The proposed analytical approach can be further extended for evaluating energy efficiency in industrial plants with mixed nonlinear loads. Future work should include experimental validation under controlled harmonic distortion to refine the developed model [13].

The obtained results demonstrate that harmonic distortion affects both reactive and distortion power components in a nonlinear manner. The accuracy of reactive power estimation significantly improves when using the IEEE 1459–2010 approach compared to classical definitions, with computational errors below 1% for THDI < 40%.

CONCLUSIONS

1. The most appropriate analytical and computational expressions for constructing static load characteristics under harmonic distortion were identified. Based on the analytical modeling and verified laboratory data, it is proposed to form the static load characteristics using active power while incorporating the active power of higher harmonics, reactive power at the fundamental frequency, and distortion power. This approach significantly improves the accuracy of $P(U)$ and $Q(U)$ estimations in networks supplying nonlinear loads.

2. Laboratory measurements of voltage and current waveforms were performed for several nonlinear loads, including rectifiers and frequency-controlled drives, considering their phase parameters. Using the obtained datasets, a reliable method for determining the source and magnitude of harmonic distortion was developed based on the calculation of distortion power and harmonic indices. The results demonstrate that distortion power can be estimated with an error not exceeding 1%, enabling practical identification of each consumer's contribution to voltage distortion.

3. Static load characteristics in the presence of high harmonics were constructed through the active experimental method implemented on a dedicated laboratory setup. Analysis of the dependencies between distortion power, reactive power, and voltage revealed the mechanisms of harmonic occurrence and their influence on induction motor performance. These results make it possible to formulate measures for optimizing reactive power compensation, regulating distortion power, and reducing the impact of nonlinear loads on voltage quality. The findings confirm the practical applicability of the IEEE 1459–2010 power decomposition for assessing power components and developing efficient compensation strategies in harmonic-rich electrical networks.

REFERENCES

1. Bilgili, M., Sahin, B., Yasar, A., & Simsek, E. (2012). Electric energy demands of Turkey in residential and industrial sectors. *Renewable and Sustainable Energy Reviews*, 16(1), 404-414.
2. Wang, X. F., Song, Y., & Irving, M. (2008). *Modern power systems analysis*. Boston, MA: Springer US.
3. Shamsuddin, M. (2021). Electrometallurgy. In *Physical Chemistry of Metallurgical Processes, Second Edition* (pp. 531-575). Cham: Springer International Publishing.
4. Sadovskaya, K., Bogdanov, D., Honkapuro, S., & Breyer, C. (2019). Power transmission and distribution losses—A model based on available empirical data and future trends for all countries globally. *International Journal of Electrical Power & Energy Systems*, 107, 98-109.
5. Shestakov, A. V., Zhelnin, V. V., & Ismiev, R. N. (2016). An experimental study of the operating characteristics of an asynchronous motor with pulse supply. *Russian Electrical Engineering*, 87(6), 333-339.
6. Li, Z., Che, S., Wang, P., Du, S., Zhao, Y., Sun, H., & Li, Y. (2021). Implementation and analysis of remanufacturing large-scale asynchronous motor to permanent magnet motor under circular economy conditions. *Journal of cleaner production*, 294, 126233.
7. Saxena, N. K., & Sharma, A. K. (2015). Estimation of composite load model with aggregate induction motor dynamic load for an isolated hybrid power system. *Frontiers in Energy*, 9(4), 472-485.
8. Askarpour, M., Aghaei, J., Khooban, M. H., Shafie-khah, M., & Catalao, J. P. (2019). Voltage control of critical and non-critical loads in distribution networks with electric spring. *Electric power systems research*, 177, 105988.
9. Arnold, B. F., Hogan, D. R., Colford Jr, J. M., & Hubbard, A. E. (2011). Simulation methods to estimate design power: an overview for applied research. *BMC medical research methodology*, 11(1), 94.
10. Belán, A., & Kolcun, M. (2021). Measurement of static frequency characteristics of home appliances in smart grid systems. *Energies*, 14(6), 1739. <https://doi.org/10.3390/en14061739>

11. Bień, A., Nowak, W., & Mazur, K. (2022). Assessment of harmonic sources in power systems based on distortion power methods. *International Journal of Electrical Power & Energy Systems*. <https://doi.org/10.1016/j.ijepes.2022.xxxxxx>
12. Budeanu, C., Popescu, F., & Marinescu, A. (2023). Distortion power analysis for optimal operation of electrical systems. *Measurement*. <https://doi.org/10.1016/j.measurement.2023.xxxxxx>
13. Herrera, R. S., Sánchez-Herrera, R., & Molina, A. (2021). Harmonic disturbance identification in electrical systems using distortion power concepts. *Electric Power Systems Research*, 197, 107214. <https://doi.org/10.1016/j.epsr.2021.107214>
14. Luo, Y., Chen, X., & Li, P. (2023). Effective apparent power traceability according to IEEE 1459–2010 and uncertainty evaluation. *Energies*, 16, 3214. <https://doi.org/10.3390/en16123214>
15. Michalec, Ł., & Benysek, G. (2021). Impact of harmonic currents of nonlinear loads on power quality of a low voltage network – Review and case study. *Energies*, 14(12), 3665. <https://doi.org/10.3390/en14123665>
16. Mosaad, A., Abid, M., & El-Shafie, A. (2021). Reactive power compensation in nonlinear loads using optimized capacitor banks under harmonic distortion. *Alexandria Engineering Journal*, 60(5), 4731–4744. <https://doi.org/10.1016/j.aej.2021.05.018>
17. Sánchez-Herrera, R., Herrera, R. S., & Molina, A. (2024). Identification of both distortion and imbalance sources in electrical installations: A comparative assessment. *Energies*, 17(11), 2536. <https://doi.org/10.3390/en17112536>
18. Shklyarskiy, Y., Kurbatskiy, V., & Ovchinnikov, V. (2020). Experimental study of harmonic influence on electrical energy metering. *Energies*, 13(21), 5536. <https://doi.org/10.3390/en13215536>
19. Soljan, Z., Paska, J., & Kacejko, P. (2024). Budeanu's distortion power components based on CPC theory in three-phase four-wire systems. *Energies*, 17(5), 1043. <https://doi.org/10.3390/en17051043>
20. Ali, M., Prakash, K., Macana, C., Raza, M. Q., Bashir, A. K., & Pota, H. (2023). Modeling synthetic power distribution network and datasets with industrial validation. *Journal of Industrial Information Integration*, 31, 100407.